

# Lawrence Berkeley National Laboratory

## Recent Work

### Title

A NEW Kit PARTIAL WAVE ANALYSIS BELOW 1 GeV Kn MASS

### Permalink

<https://escholarship.org/uc/item/2vc953qz>

### Authors

Barbaro-Galtieri, A.

Matison, M.J.

Alston-Garnjost, M.

et al.

### Publication Date

1973-06-01

Presented at the  
Conference on  $\pi\pi$  Scattering and  
Associated Topics, Tallahassee, Florida,  
March 28-30, 1973

LBL-1772  
Preprint c/

A NEW  $K\pi$  PARTIAL WAVE ANALYSIS  
BELOW 1 GeV  $K\pi$  MASS

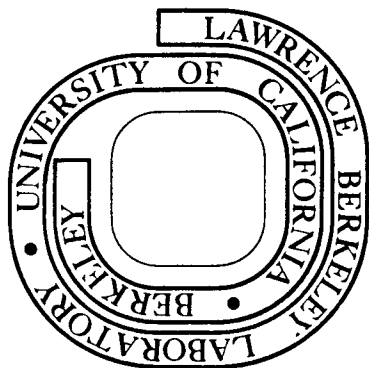
A. Barbaro-Galtieri, M. J. Matison, M. Alston-Garnjost,  
S. M. Flatté, J. H. Friedman, G. R. Lynch,  
M. S. Rabin, and F. T. Solmitz

June 1973

Prepared for the U. S. Atomic Energy Commission  
under Contract W-7405-ENG-48

**For Reference**

Not to be taken from this room



LBL-1772  
c/

## **DISCLAIMER**

This document was prepared as an account of work sponsored by the United States Government. While this document is believed to contain correct information, neither the United States Government nor any agency thereof, nor the Regents of the University of California, nor any of their employees, makes any warranty, express or implied, or assumes any legal responsibility for the accuracy, completeness, or usefulness of any information, apparatus, product, or process disclosed, or represents that its use would not infringe privately owned rights. Reference herein to any specific commercial product, process, or service by its trade name, trademark, manufacturer, or otherwise, does not necessarily constitute or imply its endorsement, recommendation, or favoring by the United States Government or any agency thereof, or the Regents of the University of California. The views and opinions of authors expressed herein do not necessarily state or reflect those of the United States Government or any agency thereof or the Regents of the University of California.

A NEW  $K\pi$  PARTIAL WAVE ANALYSIS  
BELOW 1 GeV  $K\pi$  MASS\*

A. Barbaro-Galtieri, M. J. Matison, M. Alston-Garnjost,  
S. M. Flatté,<sup>†</sup> J. H. Friedman,<sup>‡</sup> G. R. Lynch,  
M. S. Rabin,<sup>§</sup> and F. T. Solmitz

Lawrence Berkeley Laboratory  
University of California  
Berkeley, California 94720

ABSTRACT

The  $K\pi$  scattering for  $M(K\pi) < 1$  GeV has been studied in the reaction  $K^+p \rightarrow \Delta^{++}K^+\pi^-$  at 12 GeV/c incident  $K^+$  momentum. Both the moments of the  $K\pi$  angular distribution and the  $K\pi$  cross section are extrapolated to the pion pole, and the results are used in a partial wave analysis. For the s wave we have done both an energy-independent and an energy-dependent partial wave analysis. We find that only the so-called "down" solution is compatible with our data; that is, a phase shift  $\delta_0^1$  slowly increasing from  $20^\circ$  at 800 MeV to  $60^\circ$  at 1000 MeV. No evidence for an s-wave resonance near the  $K^*(890)$  mass is found, although a resonance with  $\Gamma < 7$  MeV cannot be excluded by the data. The "down" solution is well represented by an effective range formula with  $a_0^1 = -0.33 \pm 0.05$ , in good agreement with a current algebra calculation.

I. INTRODUCTION

The interest in  $K\pi$  scattering in the energy region of  $K^*(890)$  lies in the fact that some theoretical models predict the existence of an s-wave resonance at this mass. Experiments so far have failed to prove or disprove conclusively the existence of this state. Partial wave analyses of  $K\pi$  scattering in the  $K^*(890)$  region have been done by various authors.<sup>1-5</sup> The most recent analyses found two solutions for the s-wave phase shift in this mass region: a slowly varying "down" solution with  $\delta_0^1$  rising from  $20^\circ$  at 800 MeV to about  $60^\circ$  at 1000 MeV, and a rapidly rising "up" solution corresponding to a slowly varying s-wave background plus a narrow resonance ( $\Gamma \leq 30$  MeV).

\*Work done under the auspices of the U. S. Atomic Energy Commission.

<sup>†</sup>Present address: University of California-Santa Cruz, Santa Cruz, California.

<sup>‡</sup>Present address: Stanford Linear Accelerator Center, Stanford, California.

<sup>§</sup>Present address: University of Massachusetts, Amherst, Massachusetts.

Table I and Fig. 1 summarize the data used and the results obtained in these analyses. Table I shows the total number of events available to each analysis in the  $K\pi$  mass interval indicated. The number of events in the  $K\pi$  mass region below 1 GeV is much smaller, but this information is not readily available to us. It also shows the events in the incident  $K^+$  momentum region  $P_{K^+} > 8$  GeV/c. This is done because events with larger incident  $K^+$  momentum have smaller four-momentum transfer to the  $K^+\pi^-$  system and therefore are more valuable in extrapolations to the pion pole. Figure 2 shows the relation  $t_{\min}$  versus  $P_K$  for different values of  $K^+\pi^-$  masses for the reaction  $K^+p \rightarrow \Delta^{++}K^+\pi^-$ . Figure 1 shows the  $\delta_0^1$  phase shift solutions up to a mass of 1.7 GeV. In the region of  $K^*(890)$  the two ambiguous solutions are shown as obtained by the different authors.<sup>2-5</sup> This paper will only deal with  $K\pi$  scattering below 1 GeV, therefore the second ambiguity (at  $M \approx 1.5$  GeV) will not be discussed here.

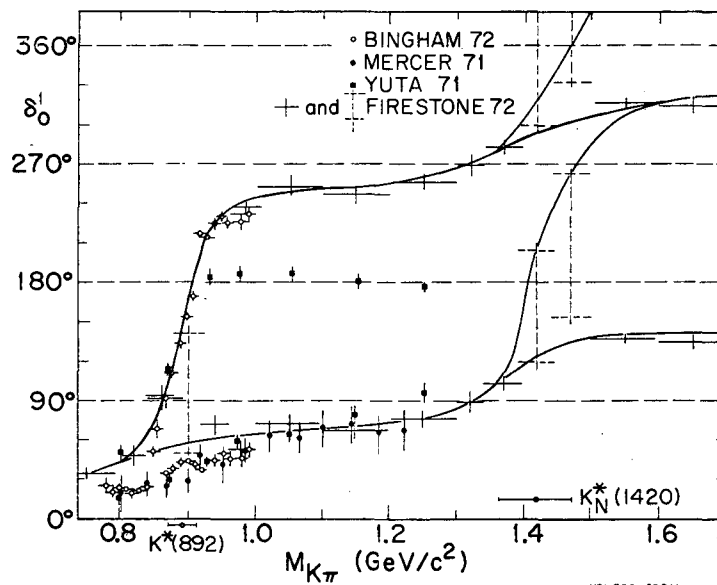


Fig. 1. Phase shift results of Bingham et al.,<sup>3</sup> Mercer et al.,<sup>2</sup> Yuta et al.,<sup>4</sup> and Firestone et al.<sup>5</sup> The curves represent possible paths connecting the ambiguous solutions as drawn by Firestone et al.

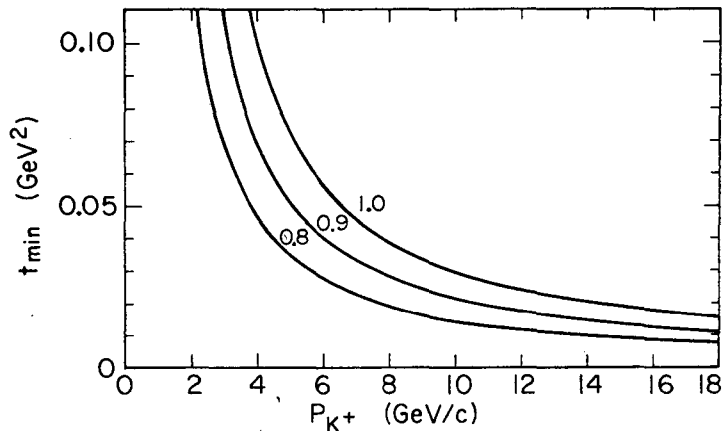
Trippe et al.<sup>1</sup> have extrapolated the total cross section to the pion pole and found only the "down" solution in the  $K^*(890)$  region; however, they suggested an s-wave resonance at about 1100 MeV. Mercer et al.,<sup>2</sup> who have used the World Data Summary Tape (WDST) compilation,<sup>6</sup> have extrapolated the  $Y_0^0$  moments to the pion pole and found both solutions. However, they eliminated the "up" solution, because it was not in agreement with the extrapolated total cross section. Bingham et al.<sup>3</sup> have also used the WDST compilation<sup>6</sup> when it included a larger number of events. They

Table I. Data used in the partial wave analysis performed by the authors indicated. The column labelled solutions refers to solutions obtained for the s wave in the  $K^*(890)$  region.

Momentum (GeV/c)	Final states	Number of events	Events in $P_K > 8$ GeV	Interval of K $\pi$ mass	Solutions	Authors
7.3	$\Delta^{++} K^+ \pi^-$	1 363		0.6-2.0	Down	Trippe et al. <sup>1</sup>
	$\Delta^{++} K^0 \pi^0$	219				
3.0-12.7	$\Delta^{++} K^+ \pi^-$	23 244	5 449	0.6-3.5	Down	Mercer et al. <sup>2, 6</sup>
	$\Delta^{++} K^0 \pi^0$	3 967	1 148			
2.5-12.7	$\Delta^{++} K^+ K^-$	31 122	12 812	0.6-3.5	Up, down	Bingham et al. <sup>3, 6</sup>
	$\Delta^{++} K^0 \pi^0$	4 845	2 667			
12.0	$\Delta^{++} K^+ \pi^-$	11 073	11 073	0.6-3.5		This experiment
5.5	n $K^+ \pi^-$	2 875		0.65-1.3	Up, down	Yuta et al. <sup>4</sup>
	p $\bar{K}^0 \pi^-$	2 086				
12.0	$K^+ \pi^- p$	2 479	2 479	0.7-2.0	Up, down	Firestone et al. <sup>5</sup>

00009300

3



XBL736-3051

Fig. 2. Minimum momentum transfer,  $t_{\min}$ , versus incident  $K^+$  momentum for the reaction  $K^+ p \rightarrow \Delta^{++} K^+ \pi^-$ . The three curves refer to the indicated values of  $K^+ \pi^-$  invariant mass.

found two solutions but disagreed with Mercer et al.,<sup>2</sup> because they found that with larger statistics the "up" solution could not be eliminated by the total cross section. The next two experiments listed in Table I have used reactions different from those of Refs. 1-3. Yuta et al.<sup>4</sup> used a one meson-exchange model neglecting absorption effects to analyze the off-mass shell  $K\pi$  scattering. They found two solutions, one of which required an s-wave resonance at  $\sim 850$  MeV. Firestone et al.<sup>5</sup> extrapolated the moments and the total cross section to the pion pole and performed a partial wave analysis which yielded two solutions as shown in Fig. 1. Recently a new method of analysis has been applied to analyze 9430 events of the reaction  $K^- p \rightarrow K^- \pi^+ n$  at 4 GeV/c by Chung et al.<sup>7</sup> They studied the mass dependence of each partial wave in the physical region without making any assumption about the nature of the production mechanism. They found that their data can accommodate little if any narrow width daughter state in the  $K^*(890)$  region.

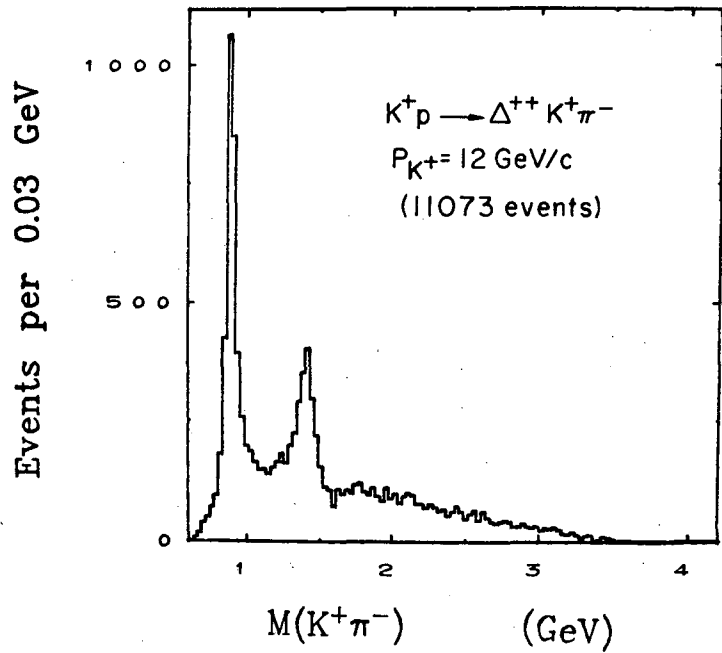
## II. THE DATA

The analysis described in this paper is based on 11 073 events of the type



with a  $K^+$  incident momentum of 12 GeV/c, obtained in an exposure of the 82-in. Hydrogen Bubble Chamber at SLAC. These events are part of the 4-prong topology of which details have been given elsewhere;<sup>8,9</sup> we only show here some important features of the data.

Figure 3 shows the  $K\pi$  invariant mass for events of reaction (1), where  $\Delta^{++}$  is defined to be  $1.16 < M(\pi^+p) < 1.36$  GeV; it shows that the distribution is dominated by  $K^*(890)$  and  $K^*(1420)$ . Figure 4 shows the momentum transfer distribution  $t_{p\Delta}$  for events of reaction (1) in the  $K\pi$  mass interval  $0.8 < M(K\pi) < 1.0$  GeV. These events are the ones to be used in the partial wave analysis reported in this paper. The  $t_{\min}$  for these events is about 0.015 (see Fig. 2); that is, they are relatively closer to the pion pole than most of the events used in previous analyses with the same reaction (see Table I and Fig. 2). In particular, a comparison with the sample of Bingham et al.<sup>3</sup> shows that we have a number of events comparable with their sample with  $P_{K^+} > 8$  GeV/c; however,  $t_{\min}$  is smaller (see Fig. 2) for most of the events in our sample. Another advantage of this experiment is that all of the events come from one exposure at one momentum in one bubble chamber, in contrast with the WDST compilation<sup>6</sup> which includes data from 14 different beam momenta, analyzed at 11 different laboratories, so that data may be subject to large uncertainties when combined.



XBL736-3048

Fig. 3. Invariant mass distribution for the  $K^+\pi^-$  system of the reaction  $K^+p \rightarrow \Delta^{++}K^+\pi^-$ . The  $\Delta^{++}$  is defined by  $1.16 < M(\pi^+p) < 1.36$  GeV.



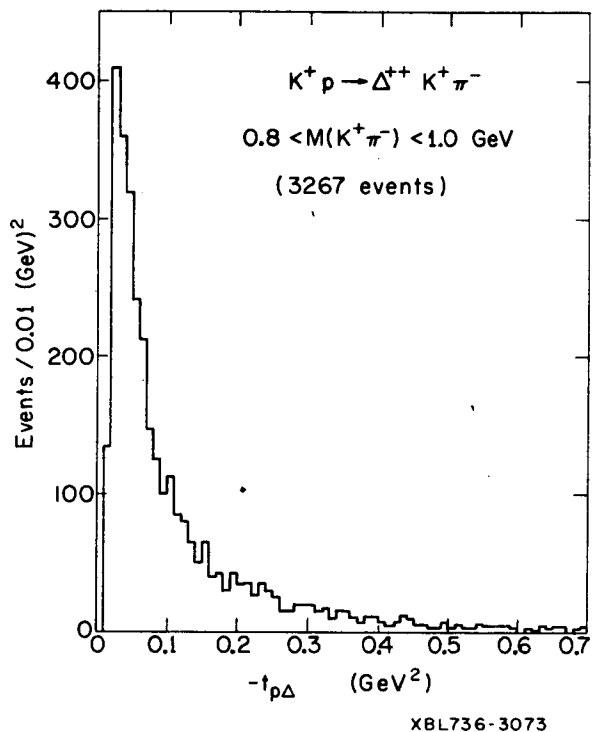


Fig. 4. Distribution of the momentum transfer squared for events of the reaction  $K^+ p \rightarrow \Delta^{++} K^+ \pi^-$  with  $K^+ \pi^-$  mass in the interval 0.8-1.0 GeV.

In order to study  $K\pi$  scattering we want to investigate the one-pion exchange process shown in the diagram of Fig. 5a. The coordinate system used to investigate reaction (1) is shown in Fig. 5b. If the one-pion exchange mechanism were dominant in our data we would expect the distributions of  $\phi_{K\pi}$  and  $\phi_{\pi p}$  angles (Treiman and Yang angles) to be isotropic. These two distributions are shown in Figs. 6 and 7 for events of the reaction  $K^+ p \rightarrow \Delta^{++} K^*$  in various momentum transfer intervals. We notice that for small  $t$  the two distributions are consistent with isotropy, whereas at large  $t$  they become anisotropic. This could be explained as the effect of background which, as expected, is larger for larger values of  $|t|$ . By doing an extrapolation to the pion pole we should be able to reduce the background to the one-pion exchange mechanism even further. We will discuss the extrapolation in the next section.

Finally, Fig. 8 shows the  $\cos\theta$  distribution for the events that we will use in the partial wave analysis; that is, events of reaction (1) with  $0.8 < M(K\pi) < 1.0$  GeV. The moments of the  $\cos\theta$  distributions for these events as well as for other  $K\pi$  mass intervals and for  $|t'| < 0.1$  GeV are shown in Fig. 9. We notice that  $Y_3 = Y_4 = 0$  for  $M(K\pi) < 1$  GeV, therefore only  $s$  and  $p$  waves are involved at these energies.

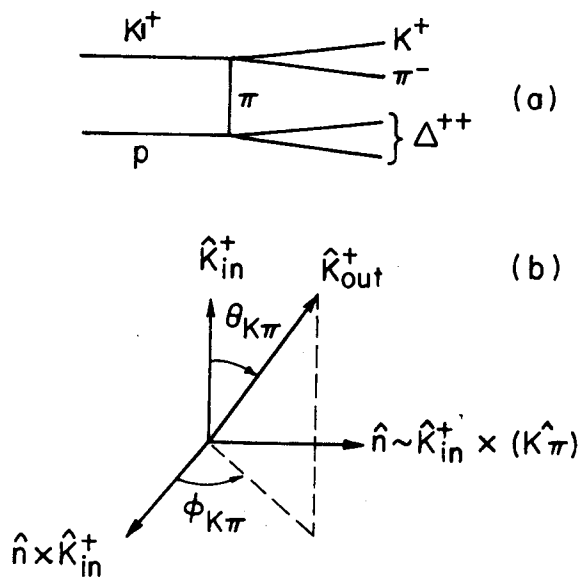
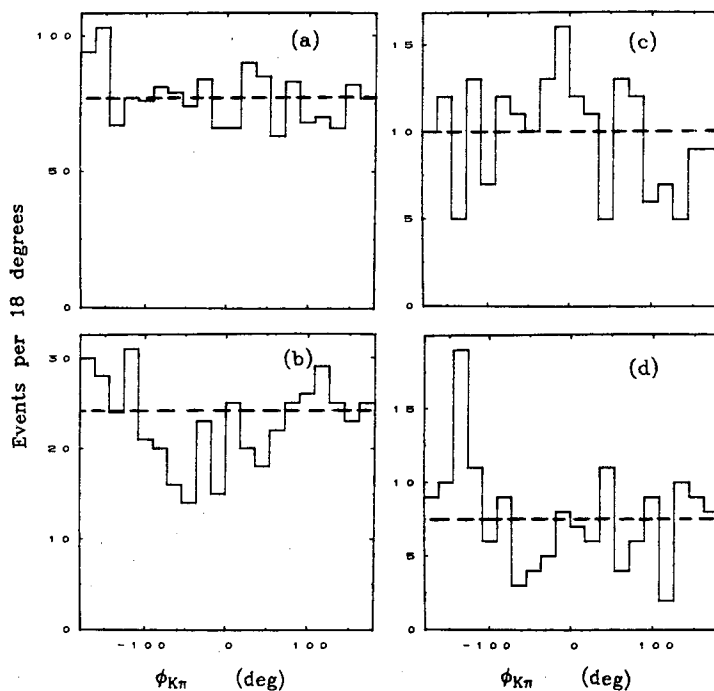


Fig. 5. (a) one-pion exchange diagram, (b) t-channel coordinate system (Jackson frame) for the  $K\pi$  vertex.  $\phi_{K\pi}$  is the Treiman-Yang angle. An analogous frame can be defined for the  $\pi p$  system.

XBL736-3049



XBL 7212-5669

Fig. 6. Treiman and Yang angle  $\phi_{K\pi}$  in the  $K^+\pi^-$  center of mass for  $K^+p \rightarrow \Delta^{++}K^*$  (890) events. (a) Events with  $|t| < 0.1 \text{ GeV}^2$  (1551); (b) events with  $|t| = 0.1$  to  $0.2 \text{ GeV}^2$  (460); (c) events with  $|t| = 0.2$  to  $0.3 \text{ GeV}^2$  (198); (d) events with  $|t| = 0.3$  to  $0.5 \text{ GeV}^2$  (156).

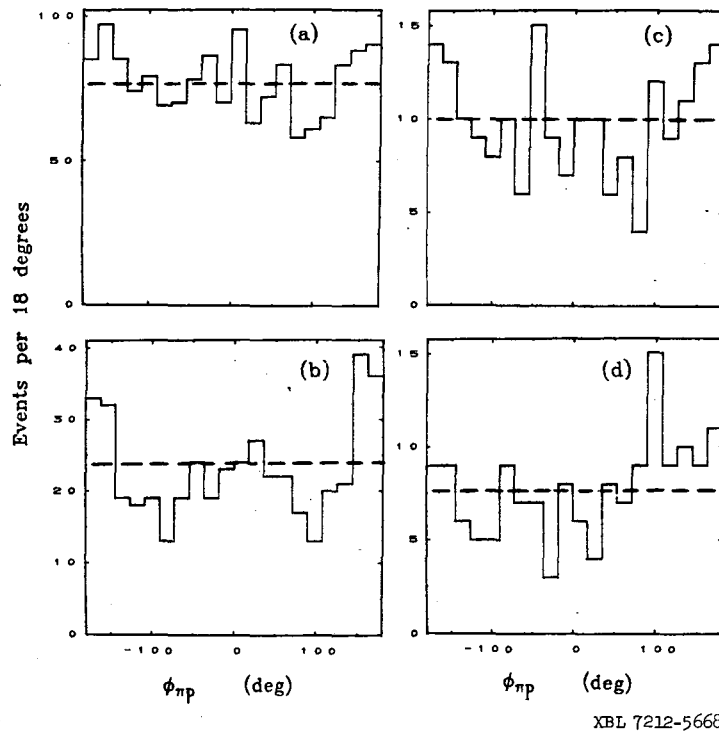


Fig. 7. Treiman and Yang angle for  $\phi_{\pi p}$  in the  $\pi^+p$  center of mass for  $K^+p \rightarrow \Delta^{++}K^*$  (890) events. (a) Events with  $|t| < 0.1$  (1685); (b) events with  $|t| = 0.1$  to  $0.2$  (370); (c) events with  $|t| = 0.2$  to  $0.3$   $\text{GeV}^2$  (185); (d) events with  $|t| = 0.3$  to  $0.5$   $\text{GeV}^2$  (131).

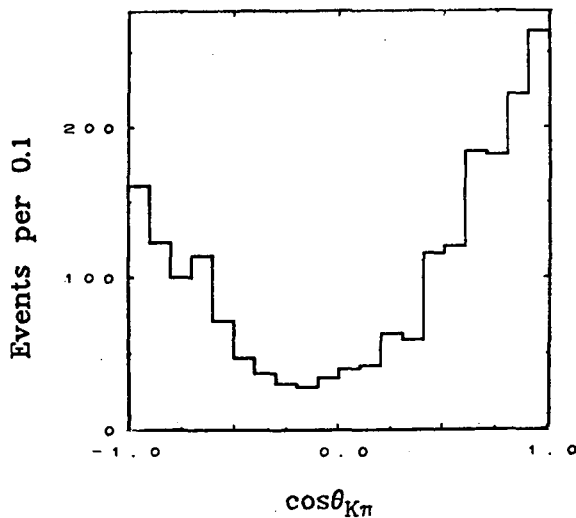
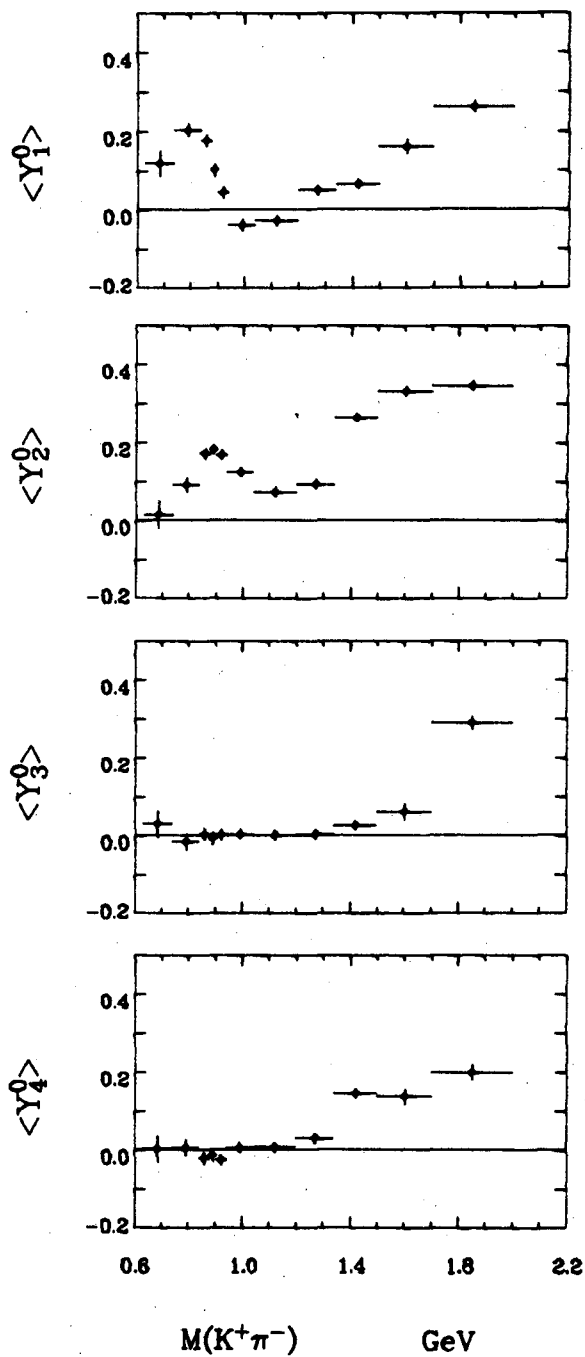


Fig. 8. Angular distribution of the  $K\pi$  scattering angle for the reaction  $K^+p \rightarrow \Delta^{++}K^+\pi^-$  for  $M(K^+\pi^-) = 0.8$  to  $1.0$   $\text{GeV}$  and  $|t| < 0.1$   $\text{GeV}^2$  (2038 events).



XBL 7212-5657

Fig. 9. Moments of the  $K^+\pi^-$  angular distribution versus  $K^+\pi^-$  mass for the reaction  $K^+p \rightarrow \Delta^+ K^+\pi^-$  for events with  $|t'| < 0.1 \text{ GeV}^2$ .

### III. EXTRAPOLATION TO THE PION POLE

#### A. Moments Extrapolation

If the differential cross section is expanded in terms of the spherical harmonics as

$$\frac{d\sigma}{d\Omega} = \frac{\sigma}{\sqrt{4\pi} a_0} \sum_{\ell=0}^{\ell_{\max}} a_{\ell} Y_{\ell}^0(\cos\theta),$$

then the expansion coefficients  $a_{\ell}$  are proportional to the "moments", i. e., the expectation values of the spherical harmonics

$$\langle Y_{\ell}^0 \rangle = \frac{a_{\ell}}{\sqrt{4\pi} a_0}.$$

We can calculate  $\langle Y_{\ell}^0 \rangle$  for the  $N$  events in a given interval of  $\pi^+p$  and  $K^+\pi^-$  mass and a given interval of  $|t|$  by estimating the expectation value:

$$\langle Y_{\ell}^0 \rangle = \frac{1}{N} \sum_{i=1}^N Y_{\ell}^0(\cos\theta_i).$$

For a chosen interval in  $\pi^+p$  and  $K^+\pi^-$  mass we calculate the values of  $\langle Y_{\ell}^0 \rangle$  in different  $|t|$  intervals. We then fit a linear  $t$  dependence  $a + bt$  for the moments in the physical region and use the parameters  $a$  and  $b$  to evaluate the moment at  $t = \mu^2 = +0.018$ , that is, at the pion-pole. The value so obtained will be referred to as the extrapolated  $\langle Y_{\ell}^0 \rangle$  moment. A quadratic extrapolation has also been done and discarded because it was not required by the data.

As a check of the extrapolation procedure we first extrapolate the  $\pi^+p$  moments for the reaction  $K^+p \rightarrow \pi^+p K^*$ , of which we have 10278 events. The extrapolated moments are shown in Fig. 10 with their errors; also shown are the experimental moments for events with  $|t'| < 0.1$  GeV.<sup>2</sup> We notice that both fit quite well to the curve calculated from on-shell  $\pi^+p$  scattering<sup>10</sup> in the mass region  $M(\pi^+p) < 1.4$  GeV. Above 1.4 GeV the calculated moments depart considerably from the extrapolated moments. As discussed previously by Schlein,<sup>11</sup> this effect is probably due to background arising from the large  $K\pi\pi$  production at  $K^*\pi$  and  $K\rho$  thresholds, the  $Q$ . Figure 11 shows the scatter plot of  $K^*\pi$  versus  $\pi^+p$  mass squared in different  $t$  intervals.<sup>8</sup> We notice that the  $Q$  is produced at every  $\pi^+p$  mass; however, it appears to be less important at small  $\pi p$  masses, especially in the  $\Delta^{++}$  region. Figure 11c shows the scatter plot for events with  $|t'| < 0.05$  GeV<sup>2</sup>; we notice that the  $Q$  is still present and that outside the  $\Delta^{++}$  region is dominant. This is again consistent with the hypothesis that the  $Q$  is the cause of the discrepancy between calculated and extrapolated moments for

$M(\pi^+p) > 1.4$  GeV. The validity of this hypothesis has been checked in a reaction where there are no strong diffraction phenomena like  $pp \rightarrow p\pi^+n$  and agreement between the high-mass  $\pi^+p$  moments and the on-shell moments was found to be very good. <sup>12</sup>

For the  $K\pi$  moments an analogous situation could arise due to a  $\Delta^{++}\pi^-$  threshold enhancement. The Dalitz plot for the  $K^+p \rightarrow \Delta^{++}K^+\pi^-$  events is shown in Fig. 12 for all events and for different  $|t'|$  intervals. Although the  $\Delta^{++}\pi^-$  enhancement is less dominant than the  $Q$ , we observe the same effect: the  $\Delta^{++}\pi^-$  enhancement is less prominent for small  $K\pi$  masses and small  $|t'|$ , and we expect it to produce small distortion of the extrapolated  $K\pi$  moments for  $K\pi$

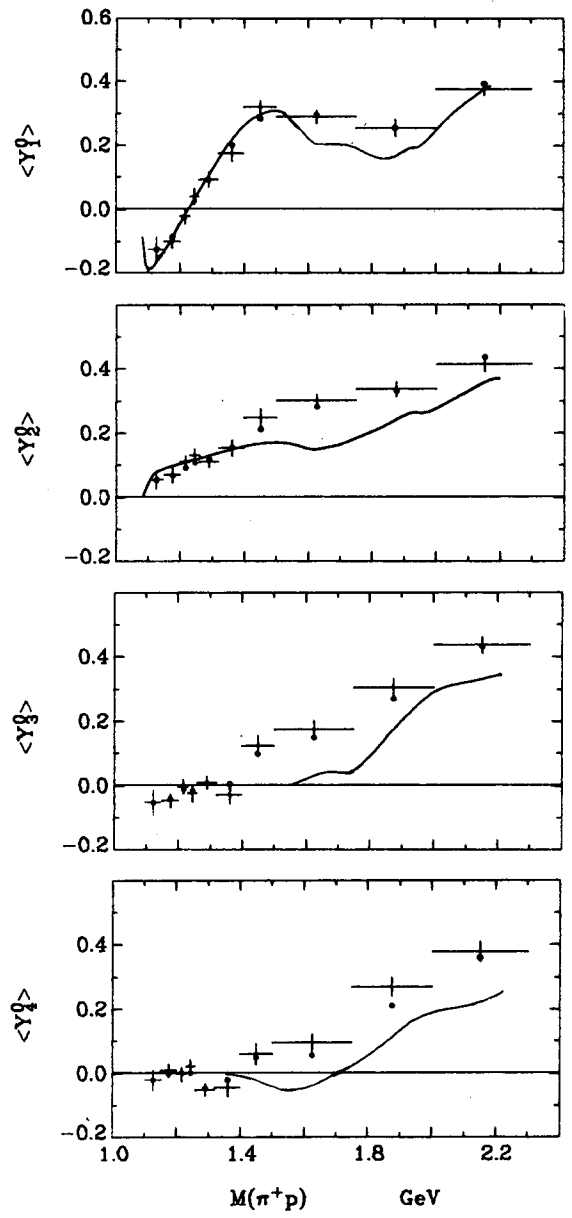
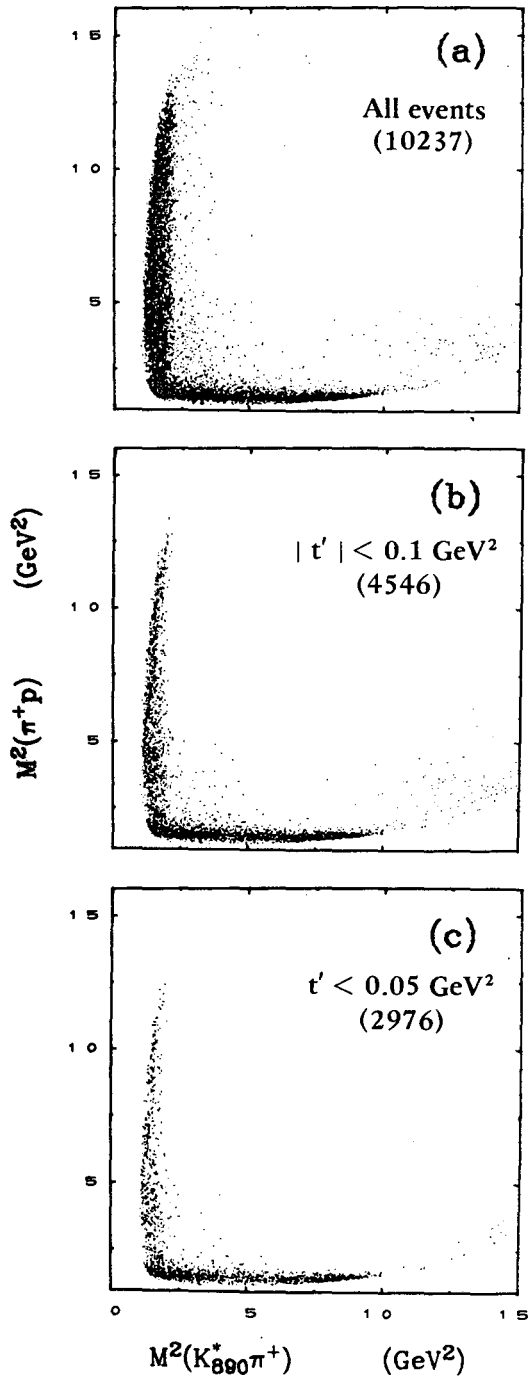
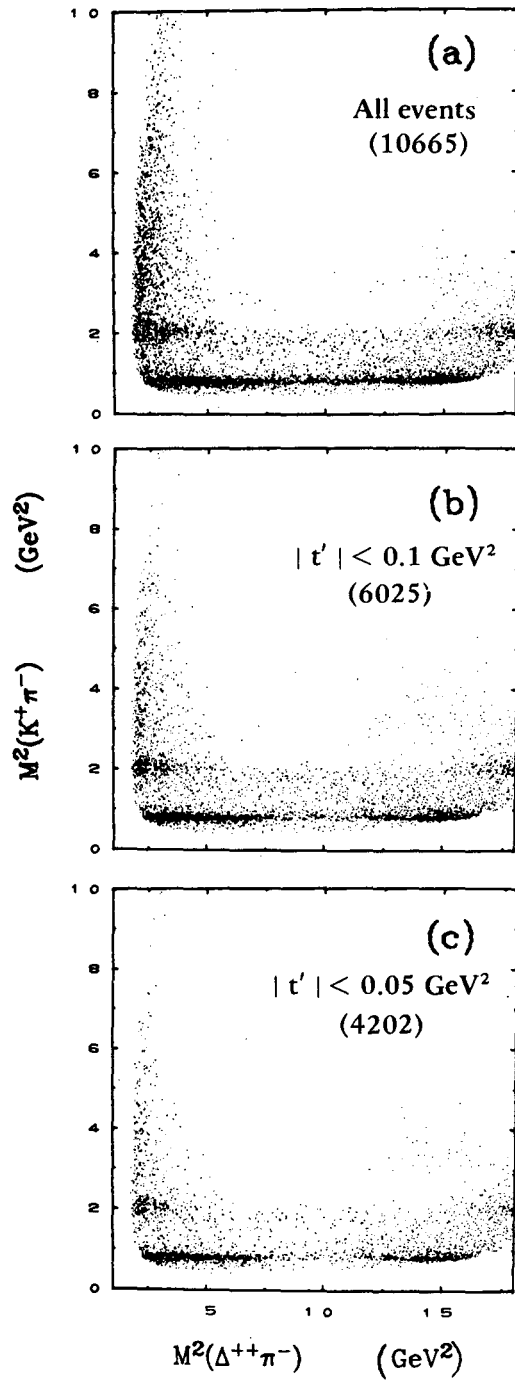


Fig. 10. Extrapolated moments of the  $\pi^+p$  angular distribution versus  $\pi^+p$  mass for events of the reaction  $K^+p \rightarrow \pi p K^*(890)$ . The dots represent the unextrapolated values; the points at the lowest  $\pi^+p$  mass are the unextrapolated values because the statistics were not enough for an extrapolation.



XBL 7212-5663

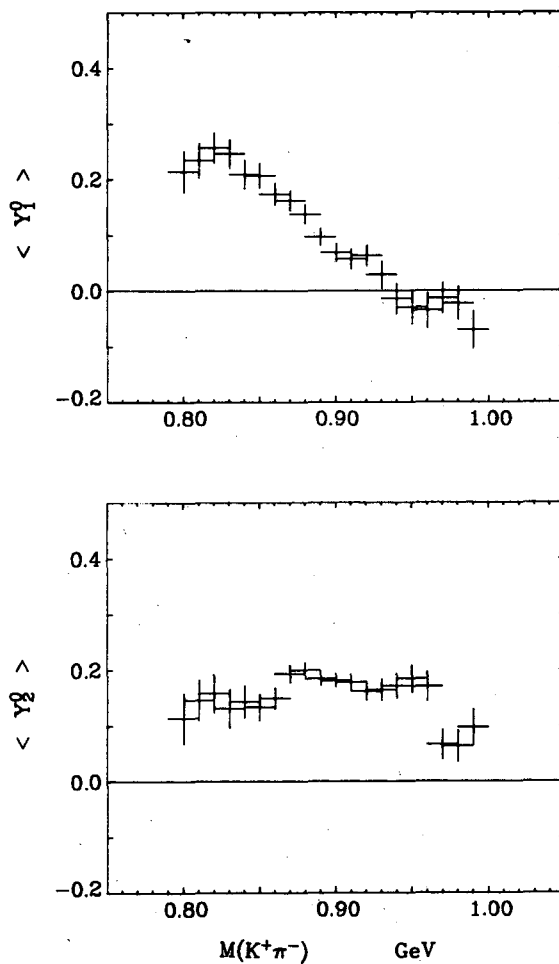


XBL 7212-5670

Fig. 11. Invariant mass squared of the  $K^*(890) + \pi$  system versus  $\pi^+p$  invariant mass squared.

Fig. 12. Invariant mass squared of the  $\Delta^{++}\pi^-$  system versus the invariant mass squared of the  $K^+\pi^-$  system.

masses below 1.4 GeV. In this paper we will be considering only  $K\pi$  masses below 1.0 GeV, where only  $Y_1^0$  and  $Y_2^0$  are different from zero, as noted in Section II. The small  $|t|$  and extrapolated  $\langle Y_1^0 \rangle$  and  $\langle Y_2^0 \rangle$  moments are shown in Figs. 13 and 14 respectively. More details on the extrapolation can be found in Ref. 9. Note that in Figs. 13 and 14 we have used overlapping  $K\pi$  bins, 20 MeV wide, whose centers are separated by 10 MeV; therefore, only one-half of the points are statistically independent.



XBL 7212-5651

Fig. 13. Moments of the  $K^+\pi^-$  angular distribution for events with  $|t| < 0.1 \text{ GeV}^2$ . Values for overlapping mass intervals are shown.



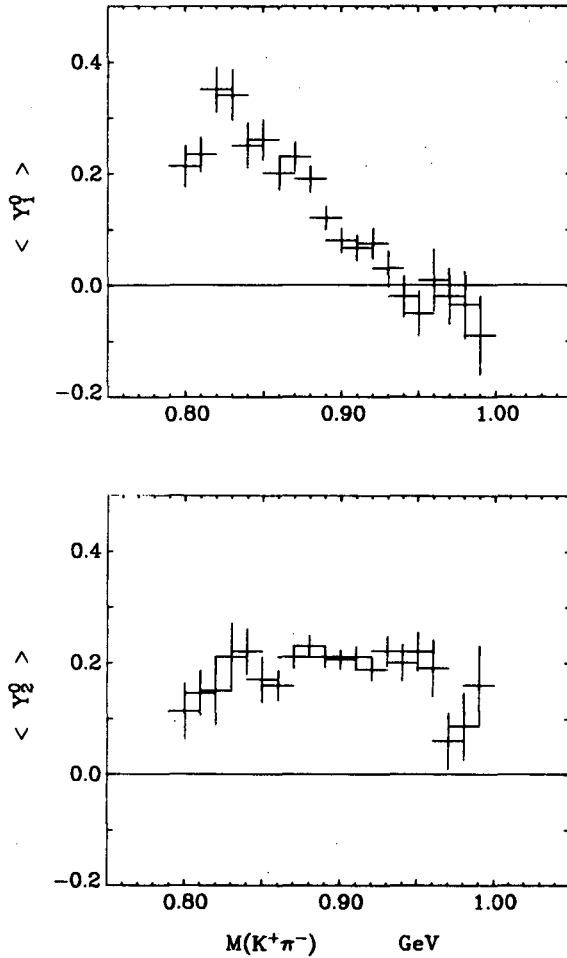


Fig. 14. Extrapolated  $K^+\pi^-$  moments. Values for overlapping  $K^+\pi^-$  mass bins are shown.

XBL 7212-5650

### B. Cross-Section Extrapolation

For the extrapolation of the total cross section we have used the Chew-Low extrapolation method<sup>13</sup> with the introduction of Dürr and Pilkuhn<sup>14</sup> (DP) form factors and the slowly varying factor  $G(t)$  introduced by Wolf.<sup>15</sup> This procedure was first used successfully by Ma et al.,<sup>16</sup> who obtained  $\pi^+p$  cross sections in the  $\Delta^{++}n$  data, in agreement with the measured  $\pi^+p$  cross sections.

For one-pion exchange the differential cross section, modified by Dürr-Pilkuhn and Wolf form factors, is

$$\frac{d^3\sigma}{dmdMdt} = \frac{1}{4\pi^3 m_p^2 P_L^2} \frac{m^2 q(m)\sigma(m) M^2 Q(M)\sigma(M)}{(t-\mu^2)^2} F(m, M, t), \quad (2)$$

where  $F(m, M, t)$  is a form factor which is 1 at the pion pole and has the form

$$F(m, M, t) = (DP)_{\pi^+ p \text{ vertex}} \times (DP)_{K\pi \text{ vertex}} \times G^2(t) \quad (3)$$

with  $(DP)_{K\pi} = 1$  for s wave,

$$(DP)_{K\pi} = \left[ \frac{q_t(m, t)}{q(m)} \right]^2 \frac{1 + R_{K^*}^2 q^2(m)}{1 + R_{K^*}^2 q_t^2(m, t)} \text{ for p wave,} \quad (4)$$

$$(DP)_{\pi^+ p} = \frac{(M+m_p)^2 - t}{(M+m_p)^2 - \mu^2} \left[ \frac{Q_t(M, t)}{Q(M)} \right]^2 \frac{1 + R_{\Delta}^2 Q^2(M)}{1 + R_{\Delta}^2 Q_t^2(M, t)},$$

$$G(t) = \frac{c - \mu^2}{c - t}.$$

Here the symbol DP is used for the Durr-Pilkhun form factors and  $G(t)$  for the slowly varying additional factor introduced by Wolf.<sup>15</sup> The remaining symbols used in Eqs. (2)-(4) are as follows:

- $m_p$  = proton mass                       $m = M(K^+ \pi^-)$   
 $P_L$  = lab beam momentum               $M = M(\pi^+ p)$   
 $\sigma(m) = K^+ \pi^-$  cross section         $\mu$  = pion mass  
 $\sigma(M) = \pi^+ p$  cross section  
 $q(m)$  is the outgoing  $K^+$  momentum in the  $K\pi$  c. m.  
 $Q(M)$  is the outgoing proton momentum in the  $\pi^+ p$  c. m.  
 $q_t(m, t)$  is the virtual  $\pi$  momentum in the  $K\pi$  c. m.  
 $Q_t(m, t)$  is the virtual  $\pi$  momentum in the  $\pi^+ p$  c. m.

The values of the numerical constants are taken to be:

$$R_{\Delta} = 3.97 \pm 0.11 \text{ GeV}^{-1},$$

$$R_{K^*} = 1.25 \pm 0.20 \text{ GeV}^{-1},$$

$$c = 2.29 \pm 0.27 \text{ GeV}^2.$$

$R_{\Delta}$  and  $c$  were obtained by Wolf,<sup>15</sup> who fitted many reactions over a large energy range. The value  $R_{K^*}$  has been obtained by Trippe et al.<sup>1</sup> by fitting data of the  $K^+ p \rightarrow \Delta^{++} K^*$  and  $K^- p \rightarrow K^{*0} n$  at various momenta between 3 and 14 GeV/c.<sup>17</sup>

For each  $K\pi$  mass interval and  $t$  interval we define a quantity

$$" \sigma_{m,t} " = \frac{(d\sigma/dt)_{\text{experimental}}}{(d\sigma/dt)_{\text{DP-OPE}}}, \quad (5)$$

where  $(d\sigma/dt)_{\text{DP-OPE}}$  stands for the integration of the right-hand side of Eq. (1) over the  $\Delta^{++}$  mass region, over the  $K\pi$  mass interval and  $t$  interval:

$$(d\sigma/dt)_{\text{DP-OPE}} = \frac{1}{4\pi^3 m_p^2 P_L^2} \int dM \int dm \int dt \frac{m^2 q(m) M^2 Q(M) \sigma(M)}{(t-\mu^2)^2} \times f(m, M, t), \quad (6)$$

with  $\sigma(M)$  taken to be the on-shell  $\pi^+ p$  cross section and  $\sigma(m)$  set equal to one. For each  $K\pi$  mass interval we calculate " $\sigma_{m,t}$ " for several  $t$  intervals, fit a straight line through these points, and calculate a value of the cross section at  $t = \mu^2$ . This value,  $\sigma_T$ , should be the on-shell  $K\pi$  cross section averaged over the mass interval under consideration, assuming that there are no rapid variations within the interval. The extrapolated cross sections, for  $K\pi$  masses below 1 GeV, are shown in Fig. 15. Also shown is the p-wave unitarity limit.

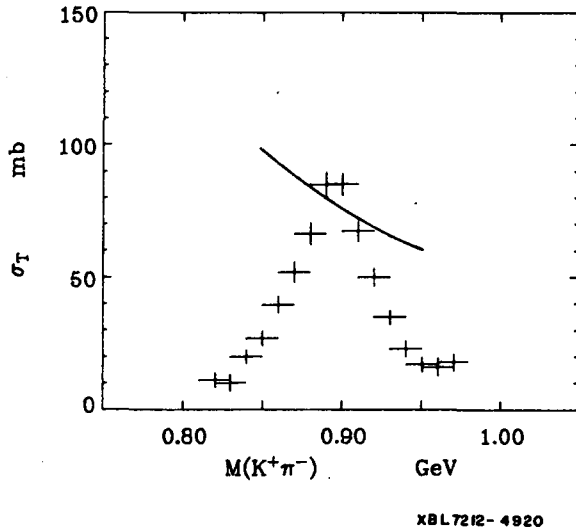


Fig. 15. Extrapolated  $K^+\pi^-$  total cross section versus  $K\pi$  mass. Values for overlapping  $K\pi$  mass bins are shown. The curve is the p-wave unitarity limit.

We have also derived the p-wave cross section from the data. Since there is no evidence for d wave at energies below 1 GeV we can write the total cross section and moments in terms of only s and p waves as follows:

$$\sigma_T = 4\pi \lambda^2 (|s|^2 + 3|p|^2) = \sigma_s + \sigma_p,$$

$$\langle Y_1^0 \rangle = \sqrt{\frac{3}{\pi}} \frac{\text{Re}(sp^*)}{|s|^2 + 3|p|^2} = \sqrt{\frac{3}{\pi}} \frac{|s| |p| \cos \phi_{sp}}{|s|^2 + 3|p|^2}, \quad (7)$$

$$\langle Y_2^0 \rangle = \frac{3}{\sqrt{5\pi}} \frac{|p|^2}{|s|^2 + 3|p|^2}.$$

The p-wave cross section is then

$$\sigma_p = \sqrt{5\pi} \langle Y_2^0 \rangle \sigma_T. \quad (8)$$

We have extrapolated to the pion pole the quantity  $\langle Y_2^0 \rangle \sigma_T$ , with the method described earlier for  $\sigma_T$ , and obtained the  $\sigma_p$  shown in Fig. 16. The curve shown is a fit with a Breit-Wigner resonance of the type

$$\sigma_p = \frac{16\pi}{3} \lambda^2 \sin^2 \delta_1^1, \quad (9)$$

with  $\cot \delta_1^1 = (m_R - m)/(\Gamma/2)$

and

$$\Gamma = \Gamma_R \frac{2 m_R}{m_R + m} \frac{q^3(m)}{q_R^3(m_R)} \frac{1 + R^2 q_R^2(m_R)}{1 + R^2 q^2(m)}.$$

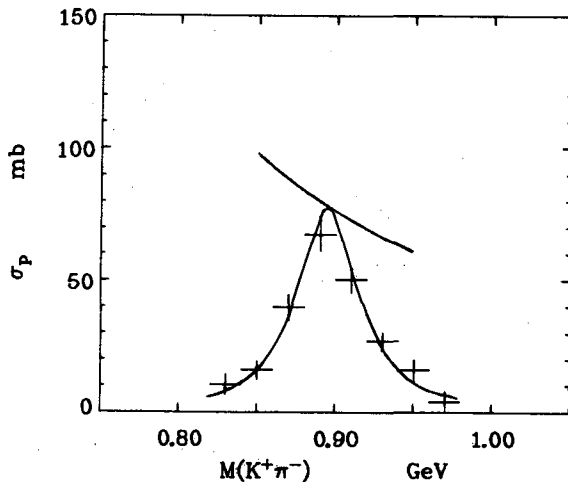


Fig. 16. Extrapolated p-wave cross section versus  $K\pi$  mass. The curve is a Breit-Wigner fitted to the data.  $M = 896 \pm 2$  MeV and  $\Gamma = 47 \pm 3$  MeV.  $\chi^2 = 5.5$  for 6 degrees of freedom.

The values obtained for the parameters are

$$m_R = 896 \pm 2 \text{ MeV},$$

$$\Gamma_R = 47 \pm 3 \text{ MeV},$$

$$R = 2 \text{ fermi},$$

in good agreement with the world average<sup>18</sup> values  $M = 896.7 \pm 0.7$  MeV and  $\Gamma = 51.7 \pm 1.0$  MeV for the neutral  $K^*$ .

#### IV. PHASE SHIFT ANALYSIS

Below 1 GeV the  $K\pi$  phase shift analysis requires only  $s$  and  $p$  waves as already mentioned in Section II. The expression for  $\sigma_T$ ,  $\langle Y_1^0 \rangle$  and  $\langle Y_2^0 \rangle$  in terms of  $s$  and  $p$  have been given in Eqs. (7). Since we are studying the  $K^+\pi^-$  channel, the isospin decomposition gives

$$s = \frac{2}{3} s_{1/2} + \frac{1}{3} s_{3/2}, \quad (10)$$

$$p = \frac{2}{3} p_{1/2} + \frac{1}{3} p_{3/2}.$$

In terms of the phase shift  $\delta_\ell^{2I}$  each partial wave is written as

$$T_\ell^{2I} = e^{i\delta_\ell^{2I}} \sin \delta_\ell^{2I} \quad (11)$$

Using only data of one charge state we do not have information on both isospin components. The  $I = 3/2$  partial waves are best studied in  $K^\pm\pi^\pm$  charge states which are pure isotopic spin states. Various authors have measured cross sections for the  $I = 3/2$   $K\pi$  system;<sup>19</sup> others have attempted phase shift analyses.<sup>20</sup> We refer to the review by Trippe<sup>19</sup> for a detailed discussion and use here the results of the analyses: the  $p_{3/2}$  was found to be very small or consistent with zero for  $M(K\pi) < 1$  GeV; the  $s_{3/2}$  wave was found to be consistent with a constant cross section, therefore with a phase shift of the form

$$\sigma_0^3 = \frac{4\pi}{q^2} \sin^2 \delta_0^3 = 1.8 \text{ mb.} \quad (12)$$

This is the form used by Bingham et al.<sup>3</sup> and is the form we use.

Using the extrapolated  $\langle Y_1^0 \rangle$ ,  $\langle Y_2^0 \rangle$  and  $\sigma_T$  values and Eqs. (7) and (10) we can perform a partial wave analysis. For the four amplitudes involved we assume that:

- a)  $s_{3/2}$  is given by expression (12) with a negative sign for the phase shift, relative to the  $s_{1/2}$  wave, as determined in Refs. 2 and 3;<sup>21</sup>
- b)  $p_{3/2} = 0$ , as discussed above;

c)  $p_{1/2}$  is parametrized as the Breit-Wigner form given by Eq. (9), as discussed in Section III-B;

d)  $s_{1/2}$  is the only unknown.

A study of other production channels in our experiment<sup>9</sup> shows that below 1 GeV the elasticity can be assumed to be one. This has also been discussed by other authors.<sup>19</sup> For a pure elastic amplitude the phase shifts of Eq. (11) are real, therefore we have only one parameter to determine,  $\delta_0^1$ . We have made both an energy-independent and energy-dependent phase shift analysis, which will be discussed next.

### A. Energy-Independent Partial Wave Analysis

To perform the partial wave analysis of the  $K\pi$  system we use as input the extrapolated quantities  $\langle Y_1^0 \rangle$ ,  $\langle Y_2^0 \rangle$  and  $\sigma_T$ , shown in Figs. 14 and 15. Therefore at each  $K\pi$  mass we have three physical quantities as input and only one unknown,  $\delta_0^1$ . For a given value of  $\delta_0^1$  we calculate a chi-square ( $\chi^2$ ) and search for a minimum of this quantity as a function of  $\delta_0^1$ . At most  $K\pi$  masses only one minimum is found, at others two minima are found. Table II shows the values of  $\delta_0^1$  corresponding to these  $\chi^2$  minima. More details can be found in Ref. 9.

The results of the analysis are shown in Fig. 17 for all  $K\pi$  mass intervals, including overlapping consecutive bins. Here we show the values of  $\delta_0^1$  corresponding to all the  $\chi^2$  minima, including the points with large  $\chi^2$ . The values of  $\delta_0^1$  for  $M(K\pi) \geq 910$  MeV are plotted for the "down" solution as well as for a "down + 180°" solution. Figure 17 shows a continuous slowly increasing "down" solution at every one of the 20 points where the analysis has been done, whereas the "up" solution is present only at two overlapping points at 890 and 900 MeV. We will discuss the two solutions separately.

1. The "down" solution has a smooth behavior in agreement with the solutions found by other authors<sup>1-5</sup> (see Fig. 1). This solution can be parametrized by an effective range formula

$$k \cot \delta_0^1 = \frac{1}{a_0} + \frac{1}{2} r_0^1 k^2, \quad (13)$$

where  $k$  is the  $K^+$  momentum in the  $K^+\pi^-$  center of mass,  $a_0^1$  is the scattering length, and  $r_0^1$  is the effective range. We have done a fit to the phase shifts of Table II, using every other entry starting at 810 MeV and found

$$\begin{aligned} a_0^1 &= -0.31 \pm 0.05 \text{ fermi}, \\ r_0^1 &= -1.4 \pm 0.5 \text{ fermi}. \end{aligned} \quad (14)$$

The fit is reasonably good, the chi-square being 10.6 for eight degrees of freedom. The phase shifts and the fitted curve are shown in Fig. 18. The value of the scattering length is in agreement with the current algebra calculation of Griffith,<sup>22</sup> who found  $a = -0.22 \pm 0.02$  fermi.

Table II.  $K^+ \pi^-$  phase shift  $\delta_0^1$  fit to extrapolated  $\langle Y_1^0 \rangle$ ,  $\langle Y_2^0 \rangle$  and  $\sigma_T$ .

K $\pi$ Mass (GeV)	"Down" solution	$\chi^2$	"Up" solution	$\chi^2$
	$\delta_0^1$ (degrees)	( $N_D = 2$ )	$\delta_0^1$ (degrees)	( $N_D = 2$ )
0.790-0.810	30 $\pm$ 7	1.0		
0.800-0.820	19 $^{+10}_{-4}$	1.0		
0.810-0.830	24 $\pm$ 4	4.6		
0.820-0.840	23 $\pm$ 4	5.3		
0.830-0.850	29 $\pm$ 5	2.4		
0.840-0.860	37 $\pm$ 5	0.1		
0.850-0.870	48 $\pm$ 6	3.0		
0.860-0.880	43 $\pm$ 6	1.7		
0.870-0.890	38 $\pm$ 5	0.6	Shoulder at 100	33.7
0.880-0.900	36 $\pm$ 4	2.7	133 $\pm$ 5	2.3
0.890-0.910	39 $\pm$ 5	3.7	151 $\pm$ 5	3.2
0.900-0.920	45 $\pm$ 4	0.9	163 $\pm$ 5	10.3
0.910-0.930	54 $\pm$ 5	0.1	164 $\pm$ 5	21.3
0.920-0.940	48 $\pm$ 5	3.6	179 $^{+7}_{-6}$	21.8
0.930-0.950	40 $\pm$ 6	1.3		
0.940-0.960	31 $^{+8}_{-16}$	2.4		
0.950-0.970	45 $\pm$ 8	3.5	187 $^{+8}_{-6}$	6.6
0.960-0.980	56 $\pm$ 7	0.4		
0.970-0.990	58 $\pm$ 9	0.1		
0.980-1.000	56 $\pm$ 9	2.5		

We searched the complex energy plane for poles of the scattering matrix and found a pole in sheet II, defined by the convention of Frazer and Hendry,<sup>23</sup> at  $M = 1062$  MeV and  $\Gamma = 470$  MeV. It is reasonable to expect such a pole, since the phase shift of Fig. 18 would cross  $90^\circ$  if it were to increase with the same energy dependence. However, since we have not used data above 990 MeV, this result is not conclusive.

2. The "up" solution is obtained only at two overlapping points, at 890 and 900 MeV. In this mass region the phase for the p-wave resonance,  $K^*(890)$ , goes through  $90^\circ$ , and Eqs. (7) show that we expect a phase ambiguity intrinsic to the analysis. In fact both  $s \cdot p$  and  $|\vec{s}|$  would be the same for a phase  $\delta_0^1 = 90 - \phi_{sp}$  and  $(\delta_0^1)' = 90 + \phi_{sp}$ . If  $s_{3/2}$  were zero this would result in a twofold

ambiguity for  $s_{1/2}$ . In practice we expect an ambiguity for  $s_{1/2}$  because  $s_{3/2}$  is small, and the statistical accuracy of our data is limited.

Our results show that the "up" solution is reduced to only two overlapping points where an ambiguity intrinsic to the analysis is expected. In addition the distributions of  $\langle Y_1^0 \rangle$ ,  $\langle Y_2^0 \rangle$  and  $\sigma_T$  as a function of  $K\pi$  mass do not show any sharp variations, which in general are associated with a narrow resonance. Therefore, there is no evidence in our data for an "up" resonant solution. However, one can still draw a continuous "up" solution by connecting the two points at 890 and 900 MeV with the "down" solution below 890 MeV and the "down + 180°" solution above 900 MeV. This would correspond to a very narrow s-wave resonance at this mass. The resolution of this experiment at the  $K^*(890)$  mass is  $\Gamma/2 = 5$  MeV;<sup>24</sup> however, we have chosen to analyze the data in 20-MeV intervals in order to have sufficient statistical accuracy for the extrapolation. In order to investigate for what width an s-wave resonance is incompatible with our data, we perform next an energy-dependent partial wave analysis.

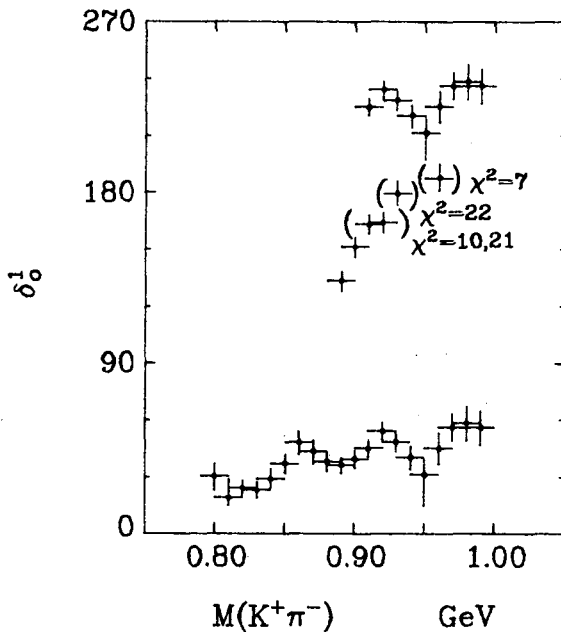


Fig. 17.  $I=1/2$ , s-wave phase shift,  $\delta_0^1$ , from an energy independent fit to the extrapolated  $\langle Y_1^0 \rangle$ ,  $\langle Y_2^0 \rangle$ , and  $\sigma_T$ .

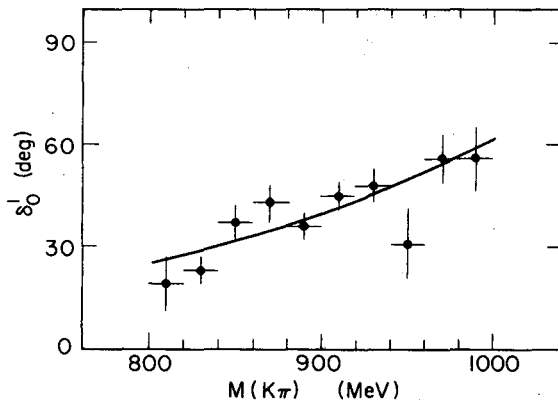


Fig. 18. Effective range fit to the phase shifts of the "down" solution.



### B. Energy-Dependent Partial Wave Analysis

We parametrize the  $s_{1/2}$  amplitude as

$$s_{1/2} = \frac{1}{\cot\delta_0^1 - i} \quad (15)$$

Since the amplitude is elastic, a simple way to combine a background and resonant amplitude preserving unitarity is to add the two phase shifts as follows:<sup>25</sup>

$$\delta_0^1 = \delta_B + \delta_R, \quad (16)$$

where  $\delta_B$  is given by Eq. (13), which fits the down solution very well, and  $\delta_R$  is the phase of an s-wave resonance of the form

$$\cot\delta_R = \frac{M_s - m}{\Gamma/2}, \quad (17)$$

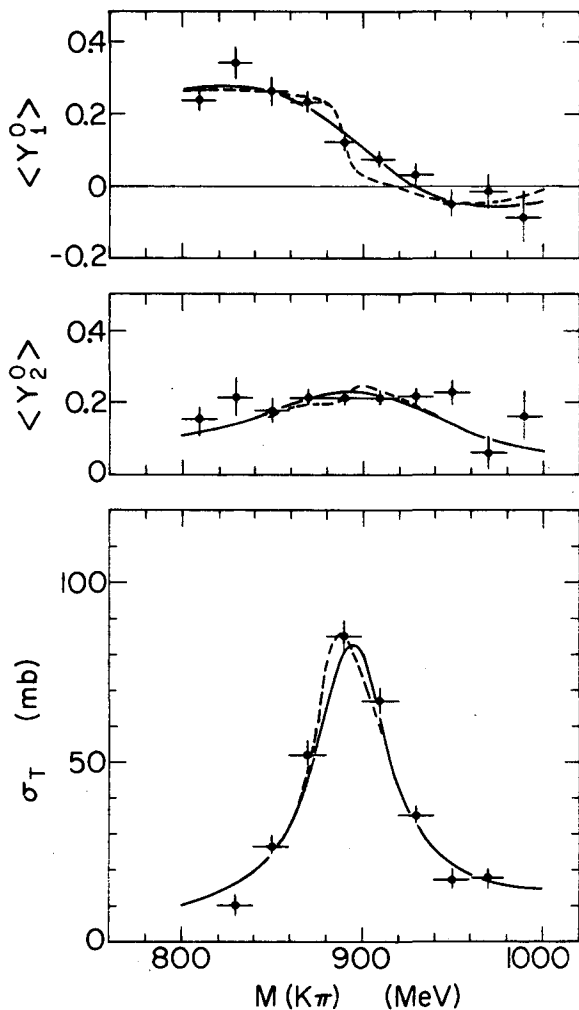
$$\Gamma = \Gamma_s \frac{2 M_s}{M_s + m} \frac{q}{q_s}.$$

Here  $M_s$  and  $\Gamma_s$  are the mass and width of the resonance,  $m$  is the  $K\pi$  mass, and  $q_s$  is the momentum of the  $K\pi$  system at the mass  $M_s$ .

If we include a resonance the s-wave amplitude has four parameters:  $a_0^1$ ,  $r_0^1$ ,  $M_s$ , and  $\Gamma_s$ . We have 30 data points as input,

$\langle Y_1^0 \rangle$ ,  $\langle Y_2^0 \rangle$  and  $\sigma_T$  at 10 different non-overlapping  $K\pi$  mass values, which we use for an overall fit. Since the data points are average values over 20-MeV mass intervals, we calculate an average of the function over 20-MeV bins and in addition we fold in the mass resolution as a Gaussian with a  $\pm 5$ -MeV width at half maximum.<sup>24</sup> For each data point we calculate in this way the expected value of the function and then calculate a chi-square. We minimize the sum of the  $\chi^2$  over the 30 data points to find values of the parameters.

We find that the non-resonant hypothesis, that is  $\delta_R=0$  in Eq. (16), fits as well as the resonant hypothesis. However, the width of the resonance for the best resonant fit is  $\Gamma_s < 1$  MeV, which we cannot detect since we have 20-MeV bins and  $\pm 5$  MeV resolution. At two standard deviations from the best resonant fit the width is  $\Gamma_s = 7$  MeV. The data used in the fit are shown in Fig. 19, where the solid curve represents the scattering length fit,  $\delta_R = 0$  in Eq. (16), and the dashed curve represents the fit for  $\Gamma_s = 7$  MeV. A resonance with this width could produce a detectable effect especially in the  $Y_1^0$  and  $\sigma_T$  distributions. The non-resonant fit gives  $a_0^1 = -0.33$ ,  $r_0^1 = -1.1$ ,  $\chi^2 = 36.0$  for 26 degrees of freedom, with parameters in agreement with the ones obtained in the energy-independent fit [Eq. (14)].



XBL736-3072

Fig. 19. Extrapolated  $\langle Y_1^0 \rangle$ ,  $\langle Y_2^0 \rangle$  and  $\sigma_T$ . The curves are the results of energy-dependent fits. The solid curve represents the best fit for the non-resonant hypothesis; the dashed curve is the fit for an s-wave resonance with  $\Gamma = 7$  MeV added to an effective range background.

## V. CONCLUSIONS

We find no evidence in our data for an s-wave resonance near the  $K^*(890)$ . In both the energy-independent and energy-dependent partial wave analysis we find that the "down" solution fits our data adequately. However, since we have limited statistics and a mass resolution of  $\pm 5$  MeV we cannot exclude an  $s_{1/2}$  resonance with  $\Gamma < 7$  MeV.

The analysis of Bingham et al.,<sup>3</sup> who used the WDST compilation data,<sup>6</sup> found two solutions that fitted the data equally well: a "down" solution similar to ours and an "up" solution corresponding to a resonance added to background with  $\Gamma \lesssim 30$  MeV. In our experiment we have a better mass resolution, and in addition we have included the total cross-section measurements in the fit, thus adding constraints in the fit. We found no "up" solution, but could not exclude one corresponding to a resonance with  $\Gamma_s < 7$  MeV. The other analyses listed in Table I with two solutions had fewer statistics than our analysis. Chung et al., who used a different method of analysis, agree with our conclusions.<sup>7</sup>

In conclusion, we find that the s-wave  $K\pi$  scattering in the 0.8- to 1.0 GeV mass region is adequately represented by a phase shift slowly varying from  $20^\circ$  to  $70^\circ$ . Its energy dependence is well represented by an effective range formula with a scattering length  $a_0 = -0.31 \pm 0.05$  fermi and an effective range  $r_0 = -1.4 \pm 0.5$  fermi. The scattering length is in agreement with the current algebra calculation of Griffith:<sup>22</sup>  $a = -0.22 \pm 0.02$  fermi.

## REFERENCES

1. T. G. Trippe et al., Phys. Letters 28B, 143 (1968).
2. R. Mercer et al., Nucl. Phys. B32, 381 (1971).
3. H. H. Bingham et al., Nucl. Phys. B41, 1 (1972).
4. H. Yuta et al., Phys. Rev. Letters 26, 1502 (1971).
5. A. Firestone et al., Phys. Rev. Letters 26, 1460 (1971).
6. The  $K^+p$  World Data Summary Tape contains events from eight different experiments conducted at eleven laboratories in Europe and the USA. See Refs. 4 and 5 for more details.
7. S. U. Chung, R. L. Eisner, and M. Aguilar-Benitez, Phys. Rev. Letters 29, 1570 (1972).
8. For further discussion of this final state see P. J. Davis et al., Phys. Rev. D 5, 2688 (1972).
9. "A study of  $K\pi$  Scattering in the reaction  $K^+p \rightarrow K^+\pi^-\Delta^{++}$  at 12 GeV/c"; by M. Matison, A. Barbaro-Galtieri, et al., Lawrence Berkeley Laboratory Report LBL-1537, to be submitted to Phys. Rev. (1973).
10. The moments were calculated from the phase shift analysis of Donnachie et al., Phys. Letters 26B, 161 (1968).
11. For a discussion of the effect of the Q bump on the  $\pi^+p$  moments see P. E. Schlein in Proceedings of the Conference on  $\pi\pi$  and  $K\pi$  Interactions (Argonne National Laboratory, 1969), p. 446.

12. E. Colton and P. Schlein, in Proceedings of the Conference on  $\pi\pi$  and  $K\pi$  Interactions (Argonne National Laboratory, 1969), p. 1.
13. G. F. Chew and F. E. Low, Phys. Rev. 113, 1640 (1959).
14. H. Dürr and H. Pilkuhn, Nuovo Cimento 40A, 899 (1965).
15. G. Wolf, Phys. Rev. Letters 19, 925 (1967).
16. Z. Ming Ma et al., Phys. Rev. Letters 23, 342 (1969).
17. P. E. Schlein, in Meson Spectroscopy, edited by C. Baltay and A. H. Rosenfeld (Benjamin, 1968), p. 161.
18. Review of Particle Properties, Particle Data Group, Rev. Mod. Phys. 45, S1 (1973).
19. For a recent review see T. G. Trippe, Recent Experimental Studies of the  $K\pi$  Interactions, in Zero Gradient Synchrotron Workshops, Summer 1971, ANL/HEP 7208, Vol. I, page 6 (1971).
20. A. M. Bakker et al., Nucl. Phys. B24, 211 (1970), and Meson Resonances and Related Electromagnetic Phenomena, edited by R. H. Dalitz and A. Zichichi (International Physics Series, Bologna, 1971), p. 53; B. Jongejans and K. Voorthuis, *ibid.*, page 57.
21. The sign can be determined only in experiments which fit both  $K^+\pi^-$  and  $K^0\pi^0$  simultaneously.
22. R. W. Griffith, Phys. Rev. 176, 1705 (1968). The values and errors for the coupling constants used to calculate this prediction have been taken from the review of G. Ebel et al., Nucl. Phys. B83, 317 (1971).

23. W. R. Frazer and A. W. Hendry, Phys. Rev. 134, B1307 (1964).
24. P. J. Davis et al., Phys. Rev. Letters 23, 1071 (1969).
25. See, for example, similar fits made for the  $\Delta^{++}(1236)$  in A. Barbaro-Galtieri, "Selected Topics in Baryon Resonances," Lectures for the 1971 Erice Summer School, Lawrence Berkeley Laboratory LBL-555 (1972).

LEGAL NOTICE

*This report was prepared as an account of work sponsored by the United States Government. Neither the United States nor the United States Atomic Energy Commission, nor any of their employees, nor any of their contractors, subcontractors, or their employees, makes any warranty, express or implied, or assumes any legal liability or responsibility for the accuracy, completeness or usefulness of any information, apparatus, product or process disclosed, or represents that its use would not infringe privately owned rights.*

TECHNICAL INFORMATION DIVISION  
LAWRENCE BERKELEY LABORATORY  
UNIVERSITY OF CALIFORNIA  
BERKELEY, CALIFORNIA 94720